Earth and Space Science

RESEARCH ARTICLE
10.1029/2021EA001855

Understanding the Dominant Moisture Sources and Pathways of Summer Precipitation in the Southeast Prairie Pothole Region

Benjamin D. Abel[1], **Balaji Rajagopalan**[1,2], **and Andrea J. Ray**[3]

[1]Department of Civil, Environmental, and Architectural Engineering, University of Colorado Boulder, Boulder, CO, USA, [2]Cooperative Institute for Research in Environmental Sciences, University of Colorado Boulder, Boulder, CO, USA, [3]National Oceanic and Atmospheric Administration, Physical Sciences Laboratory, Boulder, CO, USA

Key Points:

- Land is the primary source of moisture for all summer rainfall events in the southeast Prairie Pothole Region (SEPPR)
- The Great Plains Low Level Jet/Maya Express is the primary pathway of moisture delivery for land and Gulf of Mexico sourced events
- Insights from this work can improve the skill of SEPPR summer rainfall predictions which would be useful to resource managers in the region

Supporting Information:

Supporting Information may be found in the online version of this article.

Correspondence to:

B. D. Abel,
benjamin.abel@colorado.edu

Citation:

Abel, B. D., Rajagopalan, B., & Ray, A. J. (2022). Understanding the dominant moisture sources and pathways of summer precipitation in the southeast Prairie Pothole Region. *Earth and Space Science*, *9*, e2021EA001855. https://doi.org/10.1029/2021EA001855

Received 17 MAY 2021
Accepted 3 DEC 2021

Author Contributions:

Conceptualization: Balaji Rajagopalan
Formal analysis: Benjamin D. Abel
Methodology: Balaji Rajagopalan
Supervision: Balaji Rajagopalan
Writing – original draft: Benjamin D. Abel
Writing – review & editing: Benjamin D. Abel, Balaji Rajagopalan, Andrea J. Ray

Abstract Summer rainfall in the southeast Prairie Pothole Region (SEPPR) is an important part of a vital wetland ecosystem that various species use as their habitat. We examine sources and pathways for summer rainfall moisture, large-scale features influencing moisture delivery, and large-scale connections related to summer moisture using the Hybrid Single-Particle Lagrangian Integrated Trajectory (HYSPLIT) model. Analysis of HYSPLIT back trajectories shows that land is the primary moisture source for summer rainfall events indicating moisture recycling plays an important role in precipitation generation. The Great Plains Low-Level Jet/Maya Express is the most prominent moisture pathway. It impacts events sourced by land and the Gulf of Mexico (GoM), the secondary moisture source. There is a coupling between land, atmosphere, and ocean conveyed by large-scale climate connections between rainfall events and sea surface temperature (SST), Palmer Drought Severity Index, and 850-mb heights. Land-sourced events have a connection to the northern Pacific and northwest Atlantic Oceans, soil moisture over the central U.S., and low-pressure systems over the SEPPR. GoM-sourced events share the connection to soil moisture over the central U.S. but also show connections to SSTs in the North Pacific and Atlantic Oceans and the GoM, soil moisture in northern Mexico, and 850-mb heights in the eastern Pacific Ocean. Both types of events show connections to high 850-mb heights in the Caribbean which may reflect a connection to Bermuda High. These insights into moisture sources and pathways can improve skill in SEPPR summer rainfall predictions and benefit natural resource managers in the region.

1. Introduction

Summer rainfall plays a crucial role in the ecosystem of the Prairie Pothole Region - a vast region in the northern Midwest United States with over 2.5 million ponds (Dahl, 2014) - and it is especially crucial in the southeast Prairie Pothole Region (SEPPR, Figure 1). These ponds are preferred habitat for many different species (Batt et al., 1989; Kantrud et al., 1989; Smith et al., 1964). The two major inflows to these ponds are snowmelt and summer precipitation (Winter, 2000). In some years, snowmelt has provided nearly 90% of surface runoff (Pomeroy et al., 1998), and it acts as the first major inflow of the season. Summer precipitation, though, sustains existing ponds and is thus important for habitats throughout the warm summer months. Due to the low hydraulic conductivity of the soils in the SEPPR, precipitation primarily flows as runoff to the ponds, and even a small increase in annual precipitation can cause a large increase in pond depth (Hayashi et al., 2016). In one wetland in South Dakota, pond depth was sustained due to summer precipitation before a slow decrease to dryness later in that year (Hayashi et al., 2016). Therefore, the opposite would be expected: with less summer rainfall and higher evapotranspiration, the ponds would dry faster and negatively impact species using them as habitats. Improving the skill of forecasts would be useful to wildlife managers and others in the region.

Approximately half of the annual precipitation in the SEPPR falls in the summer (Abel et al., 2020; Rosenberry, 2003; Vecchia, 2008). For example, June, July, and August were the first, second, and fourth wettest months, respectively, from 1961-1990 at the Cottonwood Lake area in North Dakota (Rosenberry, 2003). In recent decades, summer rainfall in the SEPPR has been increasing (Bromley et al., 2020; Easterling et al., 2017). This historical increase contributes to the strong west-to-east gradient of precipitation across the SEPPR (Millett et al., 2009). Projections of summer rainfall predict no change (for RCP4.5) or a decrease of up to 10%–20% rainfall (RCP8.5) in the SEPPR (Conant et al., 2018; Easterling et al., 2017). At the same time, summer temperatures are projected to increase by 2–4°F for RCP4.5 with an even greater increase for RCP8.5 (Conant et al., 2018). This decrease of

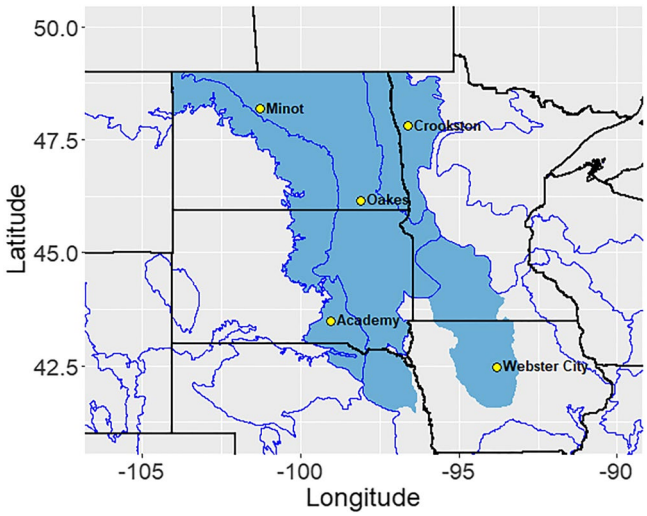

Figure 1. Map of the north-central United States, showing the southeast Prairie Pothole Region (SEPPR, in blue), the U.S. Level III Ecoregions (in blue outline), and the five weather stations (yellow circles) used in this study. The entire PPR extends north into south-central Canada; we focus on the southeastern portion in the U.S.

rainfall coupled with higher evapotranspiration due to increased temperatures would have detrimental effects on the SEPPR ecosystem.

Summer precipitation in the SEPPR is primarily a combination of small and large convective storms where the larger systems such as mesoscale convective systems (MCS) play a significant role. MCSs are prevalent during the summer producing 30%–70% of the total rainfall in the Great Plains (Fritsch et al., 1986; Haberlie & Ashley, 2019) and 76% of extreme rainfall in the northern Great Plains (Schumacher & Johnson, 2006). Song et al. (2019) found two favorable large-scale environments associated with MCSs - both have a large-scale front that extends north to south across the Great Plains and a strengthened Great Plains Low Level Jet (GPLLJ). Extreme rainfall events of the northern Great Plains frequently occur during June-September (Schumacher & Johnson, 2006), and the frequency of extreme precipitation events as well as droughts are expected to increase in the region (Conant et al., 2018; Easterling et al., 2017). This ecosystem is highly sensitive to the climate variability it experiences (Johnson & Poiani, 2016; Johnson et al., 2005, 2010), and this variability already presents challenges to wildlife management (Yocum & Ray, 2019). An increase in these extremes would only exacerbate the wildlife management issues faced by the SEPPR.

Some prior studies have provided insights into moisture sources of summer precipitation that include parts of the SEPPR, though none have specifically used the SEPPR as their target region. Brubaker et al. (2001) used a 36-year period (1963–1998) of warm-season precipitation to determine the origins of moisture for the Mississippi River basin and its subbasins. Of interest from this work are the results for the Missouri River and Upper Mississippi subbasins because they both include portions of the SEPPR. Observed precipitation was traced to its most-likely evaporative source using a back-trajectory algorithm, hourly observed precipitation, and National Centers for Environmental Prediction (NCEP) reanalysis data. Generally, they found that land was the largest contributor to summer (May 30 - August 17) precipitation. A previous study from these authors using similar methods similarly found that land was the primary source for June and July precipitation events during the drought of 1988 and flood of 1993 (Dirmeyer & Brubaker, 1999). In another study, analysis of May-July precipitation events from 1979-2007 for a portion of the Midwest (capturing the southern part of the SEPPR) shows a large portion of events sourced by land (Dirmeyer & Kinter III, 2010). A study from the same two scientists analyzed warm-season Midwest floods from 1993 (June and July) and 2008 (May and June) and found that both had moisture sourced from the south coming all the way from the Gulf of Mexico in an atmospheric river (AR) colloquially called the ”Maya Express” (Dirmeyer & Kinter III, 2009). Though ARs from the Gulf of Mexico have been shown to be most prevalent during the cold season (Debbage et al., 2017; Lavers & Villarini, 2013), studies in addition to Dirmeyer and Kinter III (2009) have noticed the impact of the ”Maya Express” in bringing moisture from the Gulf of Mexico to the Great Plains during the summer (Knippertz & Wernli, 2010; Lavers & Villarini, 2013).

With land being identified as a major source of moisture for summer precipitation in previous studies, it follows that soil moisture plays an important role in SEPPR summer precipitation development. Some previous studies have found connections between soil moisture and precipitation in the Great Plains including the SEPPR (Koster et al., 2004; Meng & Quiring, 2010; Yoon & Leung, 2015). Yoon and Leung (2015) note the memory of soil moisture (i.e., its ability to persist) and found a significant link between moisture in April and evaporation in June. They noticed high soil moisture anomalies persisted from April to June, which caused an increase in evapotranspiration, and consequently increased precipitation in June. Spring soil moisture and summer precipitation are connected via statistically significant positive correlations in much of the SEPPR (Meng & Quiring, 2010). However, they also noticed that a strong sea surface temperature (SST) influence on precipitation would mask the importance of soil moisture on summer precipitation. Finally, a strong land-atmosphere coupling between summer soil moisture and precipitation was observed in the Great Plains by Koster et al. (2004). Using an ensemble of numerical models, they noticed a significant portion of the precipitation variance was explained by soil moisture variance from 6 days prior.

The importance of the SEPPR to wildlife, the importance of summer precipitation to its ecosystem, and the projected SEPPR rainfall changes motivate the need to understand the moisture sources and pathways that deliver summer rainfall in this region. The literature summarized above largely focuses on individual events/years or on a short duration. In this paper, we build on that work and systematically examine the moisture sources and pathways for summer precipitation and extremes in the SEPPR. More specifically, we investigate the amount of summer moisture delivered by major sources, large-scale circulation features that influence summer moisture delivery, and large-scale connections related to summer moisture. These insights will be of help in improving seasonal rainfall forecasts and understanding and projecting moisture track changes and consequently, summer rainfall characteristics under future climate change and variability.

The paper is structured as follows. First, we briefly describe the data used followed by our methods in obtaining moisture source and trajectories for all rainfall days. We follow this by investigating the teleconnections to the large-scale ocean and atmosphere circulation features that influence summer moisture delivery. Results from our analysis and their discussion in a broader context and utility conclude the paper.

2. Study Region and Data

2.1. Daily Precipitation Data

We obtained daily precipitation data for five stations within the southeast Prairie Pothole Region (SEPPR, Figure 1) from the Global Historical Climatology Network (GHCN) (Durre et al., 2008, 2010; Menne et al., 2012). We chose these stations based on the following criteria. We first narrowed possible stations by longevity, keeping those with at least 90 years of records. Then, we wanted a representation of all four Level III Ecoregions of the United States (Omernik & Griffith, 2014) that span the SEPPR. In conjunction with ecoregion representation, we wanted a spatial representation of the SEPPR. Webster City, Iowa represents the Western Corn Belt Plains ecoregion. Oakes, North Dakota and Minot, North Dakota represent the Northern Glaciated Plains ecoregion. Crookston, Minnesota represents the Lake Agassiz Plain ecoregion. Academy, South Dakota represents the Northwestern Glaciated Plains ecoregion.

2.2. North American Regional Reanalysis

Gridded atmospheric data are required to compute trajectories with the Hybrid Single-Particle Lagrangian Integrated Trajectory (HYSPLIT) model. We used the National Centers for Environmental Information (NCEI) North American Regional Reanalysis (NARR) model (Mesinger et al., 2006) data from 1979-2017. We chose these data because they had the best combination of spatial resolution and temporal availability from the data sets packaged with HYSPLIT.

2.3. Large-Scale Correlation Map Variables

We used the International Research Institute's (IRI) Data Library, which compiles raw data from various sources into a common format, to retrieve SST and 850-mb height data for correlation maps eliciting large-scale climate connections. The SST data are a combination of Kaplan et al. (1998) and Reynolds and Smith (1994). The 850-mb data are from National Oceanic and Atmospheric Administration's (NOAA) Climate Data Assimilation System I (CDAS- 1) data (Kalnay et al., 1996). For Palmer Drought Severity Index (PDSI) data, we use the self-calibrated version (Dai et al., 2004) from NOAA Physical Sciences Laboratory (PSL) Climate Data Repository. Detailed information on these data can be found in Table S1 in Supporting Information S1.

We use PDSI, 850-mb heights, and SSTs to represent the lithosphere, atmosphere, and hydrosphere, respectively - primary sub-systems of the Earth system. Though PDSI uses precipitation information in its calculation, we use it as a surrogate for land because soil moisture data is lacking both temporally and spatially. In addition, PDSI is widely used, and therefore wildlife managers and other stakeholders in the SEPPR are familiar with it.

Table 1
Number of Days for Each Event Type, Count of Two- and Three-Day Precipitation Events, and the Breakdown by Source for Each Station in Summer (June, July, August, September) From 1979 to 2017

Station	Rain days	Two-day events	Three-day events	Extreme rain days	Two-day events	Three-day events
Webster City, IA	1152	361	118	141	13	0
Crookston, MN	968	250	58	140	6	1
Oakes, ND	773	166	46	87	6	0
Minot, ND	956	270	78	146	6	0
Academy, SD	902	234	66	129	5	0

	Rain			Extreme		
Station	Land	Gulf of Mexico	Pacific	Land	Gulf of Mexico	Pacific
Webster City, IA	969	179	4	107	33	1
Crookston, MN	917	46	5	123	17	0
Oakes, ND	719	51	3	76	10	1
Minot, ND	917	35	4	130	16	0
Academy, SD	840	60	2	106	23	0

3. Methods

3.1. Rain Events

We used the GHCN station data to determine dates of rain and extreme events during the summers (June, July, August, and September) from 1979-2017. We defined summer as June-September because the wet season in the SEPPR begins in spring and extends into September (Abel et al., 2020). We determined the 90th quantile precipitation amount from the subset of days with precipitation for a station. Days with precipitation amount less than or equal to the 90th quantile but greater than 1 mm were designated as rain days (henceforth "rain events"). Days with precipitation amount greater than the 90th quantile were designated as extreme rainfall events (henceforth "extreme events"). In literature, there is a wide range of what is designated as "extreme." Jana et al. (2018) use the 85th percentile while Schumacher and Johnson (2006) use events with only a 2% probability of occurrence. We therefore believe the 90th quantile represents the extreme events appropriately. The number of days per each event and the count of days by source is in Table 1.

3.2. Back Trajectories—The HYSPLIT Model

The HYSPLIT model (Draxler, 1999; Draxler & Hess, 1997, 1998; Stein et al., 2015) was used to calculate air parcel trajectories from the station of origin backward in time (henceforth "back trajectories"). These back trajectories were then used to determine the moisture source location for their associated precipitation event.

HYSPLIT was developed by the National Oceanic and Atmospheric Administration's (NOAA) Air Resources Laboratory to compute air parcel trajectories and particle transport, dispersion, chemical transformation, and deposition simulations. It has been used in other studies to identify moisture sources (e.g., Bracken et al., 2015; Gustafsson et al., 2010; Jana et al., 2018). It calculates the change in position of a parcel from the average of initial and first-guess three-dimensional wind velocity vectors (Draxler & Hess, 1998).

Multiple back trajectories were calculated with HYSPLIT starting on the dates defined as rain events or extreme events originating at the latitude and longitude of the weather station. Back trajectory position was calculated at one-hour intervals. The exact time of the rain event is not known from the GCHN daily precipitation data, so back trajectory calculations were initiated every 6 hr on the day of the event from 00:00 to 24:00. Since much of the moisture that fuels SEPPR rainfall during summer resides at lower levels (Benton & Estoque, 1954; Higgins et al., 1997; Mo et al., 2005), we select the 1,500 m level, which falls in the average range of heights for 850-mb (National Oceanic and Atmospheric Administration, 2021), for our analysis - similar to others (Izquierdo

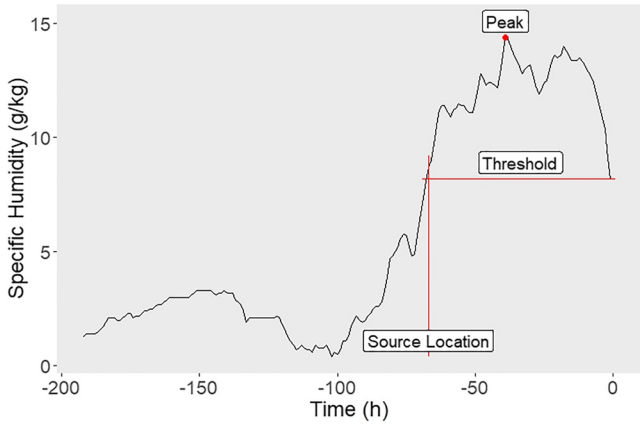

Figure 2. Illustration of how moisture source location is determined using an example trajectory. The source location is the location of the parcel at the time when the humidity is below the threshold value.

et al., 2012; Jorba et al., 2004). We calculated the back trajectories to 8 days (192 hr) prior because this is the approximate upper limit on the residence time of moisture in the atmosphere (Trenberth, 1998).

3.3. Trajectory and Moisture Source Selection

We chose one trajectory per day of the event to represent the trajectory of moisture delivery for that precipitation event then determined moisture source from the selected trajectory. We took the set of trajectories per day and determined the trajectory that had the largest drop in specific humidity before the time of event (hour 0). To determine the drop in specific humidity for each trajectory, we search backward in time from hour 0 for the peak value as long as the specific humidity does not drop below what it was at hour 0 (henceforth "threshold value"). We take the peak value minus the threshold value to determine the drop in specific humidity. With the trajectory with the highest drop in specific humidity identified, we determine the time when the parcel's specific humidity drops below the threshold value and use this location as the moisture source. Figure 2 illustrates this process using an example trajectory. If the specific humidity never drops below the threshold, the moisture source location is set as the parcel's location eight days prior.

This methodology does not separate multi-day precipitation events from single-day events. For completeness, we include the number of two- and three-day events present in our analysis in Table 1. We also provide the source count of 2- and 3-day events in Table 2. These counts were calculated from the subset of days that were selected as rain and extreme days (i.e., all days in a 2- or 3-day event meet the thresholds described in Section 3.1). In addition, two-day and three-day events were counted separately; 3-day events consist of two separate 2-day events. These multi-day events are generally a low percentage of the total events included in our analysis. The largest percentages occur for 2-day rain events where they contribute from 22%-31% of all events.

Table 2
Count of Sources for Two- and Three-Day Precipitation Events for Each Station in Summer (June, July, August, September) From 1979 to 2017

	Rain					
	Two-day events			Three-day events		
Station	Land	Gulf of Mexico	Pacific	Land	Gulf of Mexico	Pacific
Webster City, IA	306	55	0	99	19	0
Crookston, MN	232	17	1	51	7	0
Oakes, ND	143	22	1	39	6	1
Minot, ND	258	11	1	76	2	0
Academy, SD	220	12	2	65	0	1
	Extreme					
	Two-day Events			Three-day Events		
Station	Land	Gulf of Mexico	Pacific	Land	Gulf of Mexico	Pacific
Webster City, IA	10	3	0	0	0	0
Crookston, MN	6	0	0	1	0	0
Oakes, ND	5	1	0	0	0	0
Minot, ND	5	1	0	0	0	0
Academy, SD	4	1	0	0	0	0

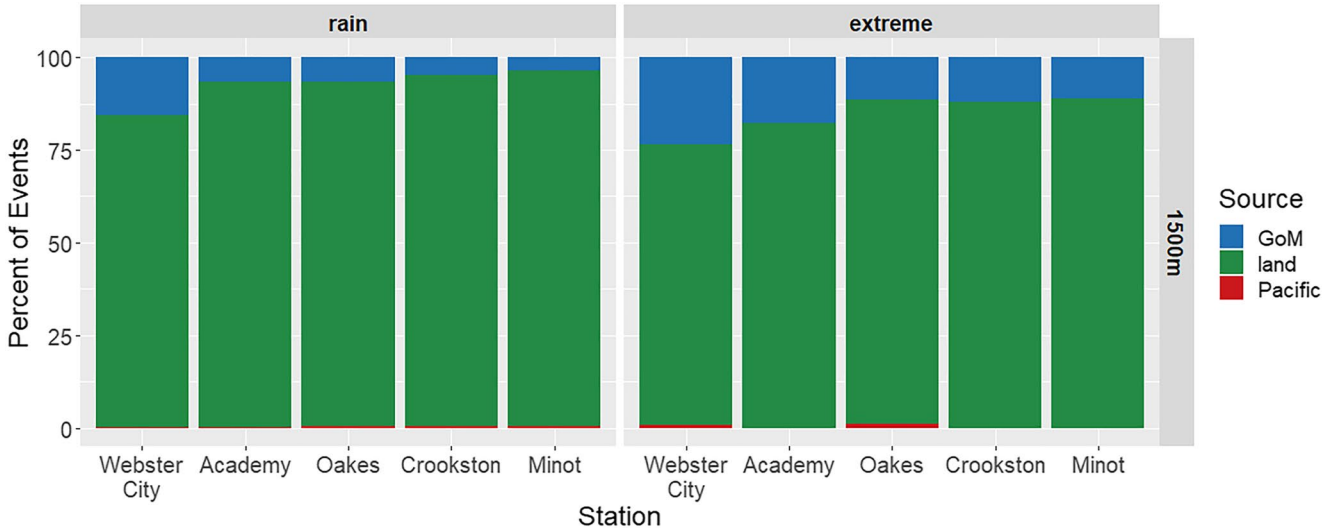

Figure 3. Percent trajectories from each source separated by the station for rain and extreme events at 1,500 m.

4. Results

For all the rainy days during summer for the period of 1979–2017 at the five selected stations (Figure 1), we ran the HYSPLIT model and analyzed the output back trajectories for their source, pathway, precipitation amount by source, and preliminary large-scale circulation and large-scale moisture setup. The results of this analysis described below, help us arrive at our conclusions for moisture delivery into the SEPPR.

4.1. Moisture Sources and Pathways

Moisture trajectory sources for each station, determined using the latitude and longitude of the source location, are displayed as percentages in Figure 3. Three sources were identified - the Gulf of Mexico (GoM), Pacific Ocean (Pacific), and land. Most events (over 75%) have land as their source location. Trajectories originating at 1,500 m have the GoM as their secondary source (from 5% to 25%), and the Pacific has nearly zero trajectories as its source. Extreme events have more trajectories originating from the GoM than rain events at the same height. The presence of two- and three-day events in these results could impact these percentages slightly, but only significantly for the percentages between land and the GoM. For example, a three-day event may present as a GoM-sourced event for the first two days then as a land-sourced event for the third day. However, since these multi-day events only account for a maximum of 31%, they would not change the overall ranks of the three moisture sources.

The distribution of percentages in Figure 3 also guides our successive presentation of results. Webster City and Minot represent the two extreme cases with the other three stations representing the range between. We, therefore, present further analysis only at these two stations and place any remaining in the Supporting Information S1. Further, it is evident that the GoM plays a larger role than the Pacific, so we will not present pathways for Pacific events.

We use areal density plots to examine prominent pathways for moisture from both land-sourced trajectories and GoM-sourced trajectories for Webster City (Figure 4) and Minot (Figure 5). The density is plotted using the stat_density2d() function in R which calculates the 2-dimensional kernal density estimate based on bivariate normal distributions. The density is scaled so that the integral of density over all points is equal to 1. Please see the function documentation for further details.

The areal density plots for Webster City's land-sourced precipitation events show a major cluster of trajectories near the station, but also show a clear pathway extending west and south for rain events (Figure 4a) and, more prominently, for extreme events (Figure 4b). For the GoM-sourced events, the major pathway extends south to the Gulf of Mexico (Figures 4c and 4d). Unlike the land-sourced events, the GoM-sourced events have higher

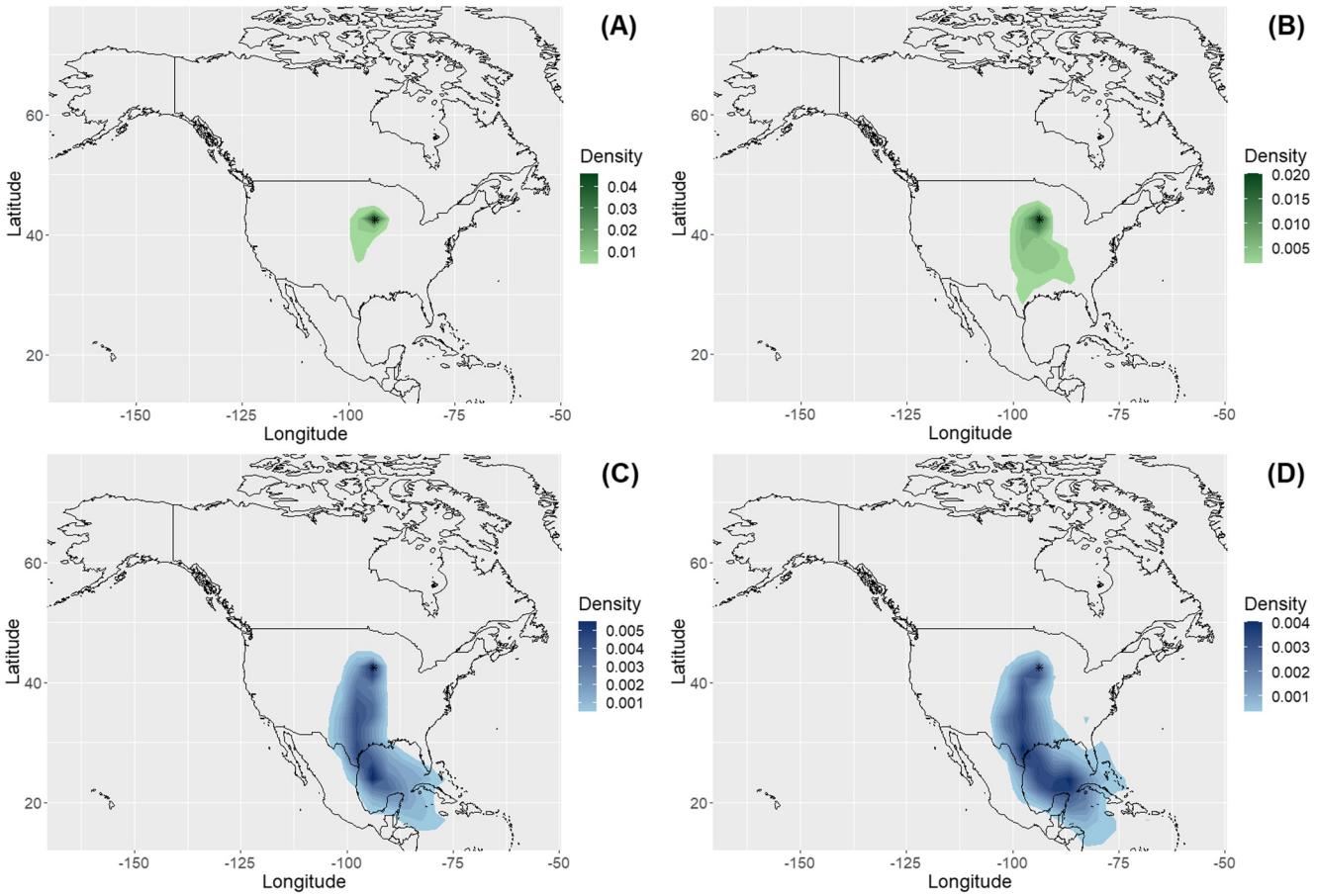

Figure 4. Density maps of Webster City trajectories with land (green) and Gulf of Mexico (blue) as their source for rain (a), (c) and extreme (b), (d) events at 1,500 m. The station location is marked with a black asterisk.

concentrations of trajectories further south along the pathway from the Gulf of Mexico. They are even denser and extend further south for extreme events (Figure 4d).

Minot's areal density plots for land-sourced precipitation events show the highest concentration of trajectories near the station (Figure 5). Trajectories have plumes close to the station with a pathway from the northwest for rain events (Figure 5a) and southeast for both rain and extreme events (Figures 5a and 5b). The GoM-sourced events have a plume that extends down to the Gulf of Mexico with the highest concentrations along this path (Figures 5c and 5d); the plume is a nearly direct pathway from the Gulf of Mexico to the station (Figures 5c and 5d) similar to those at Webster City.

4.2. Precipitation Amount by Source

To investigate the connection between moisture sources and rainfall amounts, we use boxplots of the daily rainfall amounts (both rain and extreme events) separated by station for the two primary sources, land and the GoM (Figures 6 and 7). For rain events, GoM-sourced daily precipitation amounts are higher overall and more variable than those of land-sourced events (Figure 6). Oakes is the exception as the rainfall amounts are only higher, not more variable. However, extreme events do not follow this same pattern (Figure 7). At Minot and Webster City, the land-sourced events produce higher and more variable rainfall amounts than the GoM-sourced events. At Crookston and Oakes, GoM-sourced events produce higher precipitation amounts but are not more variable. At Academy, the median rainfall amount for GoM-sourced events is higher, but the variability is nearly the same.

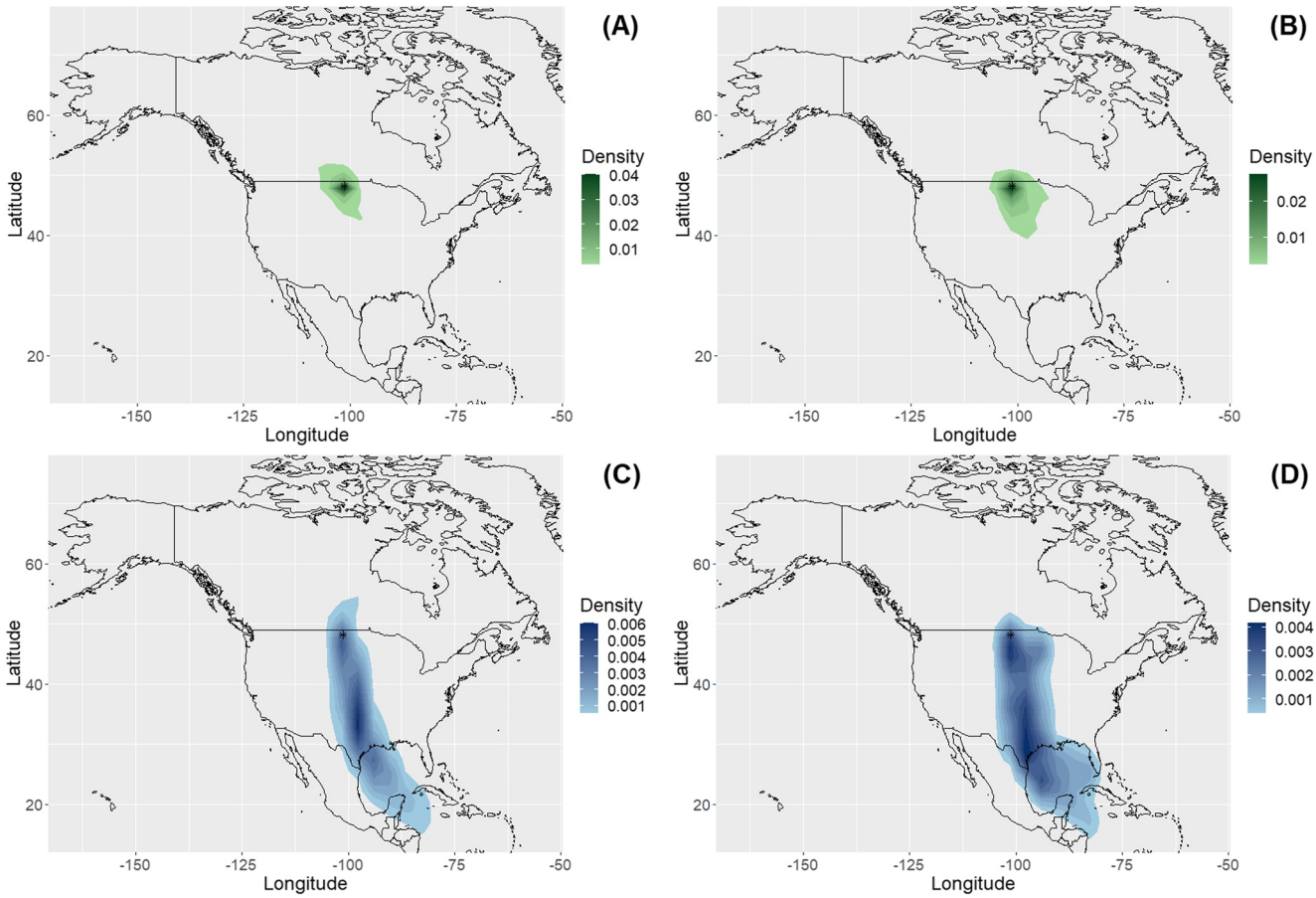

Figure 5. As in Figure 4 but for Minot.

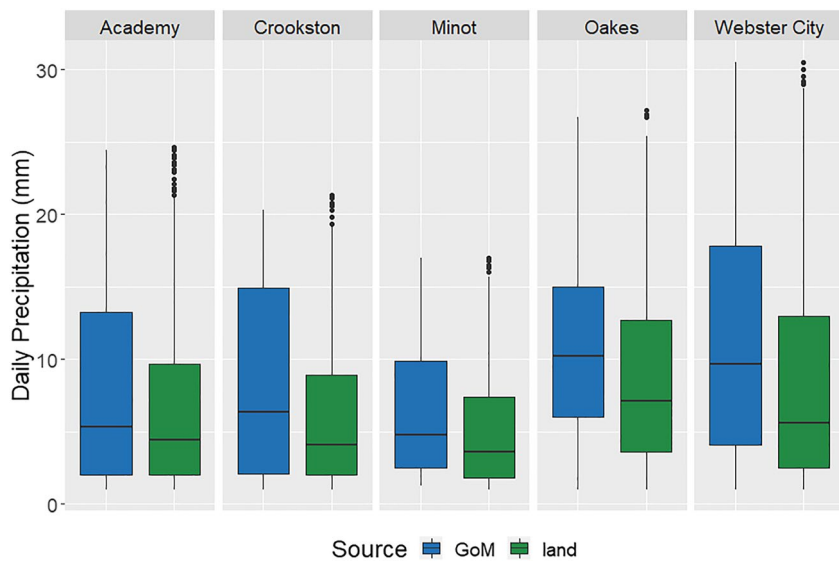

Figure 6. For back trajectories originating at 1,500 m, boxplots of daily precipitation amounts by source per station for days determined to be rain events.

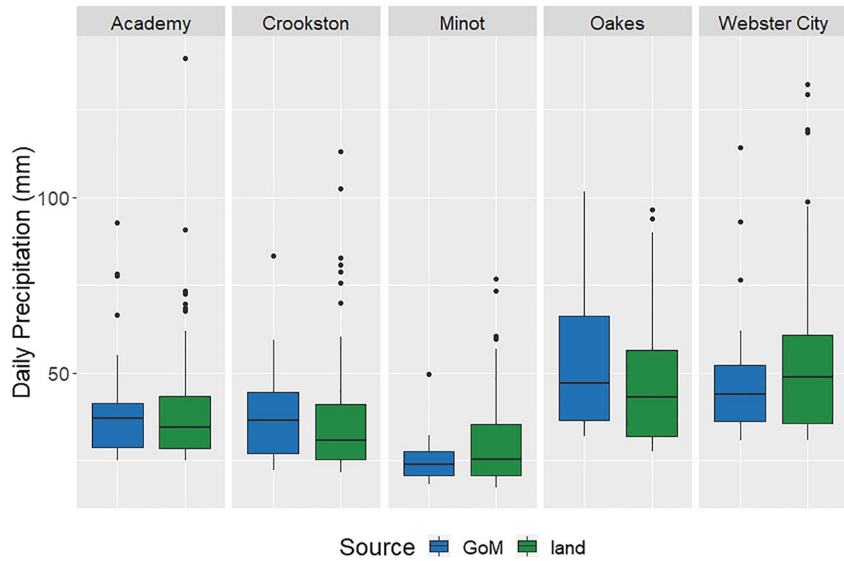

Figure 7. As in Figure 6 but for extreme events.

4.3. Large-Scale Circulation and Large-Scale Moisture Setup for Extreme Events

To understand the circulation features associated with the extreme rain events, we examine daily composites of anomalies of some large-scale circulation and moisture variables - 850-mb heights, 850-mb winds, precipitable water (PW), and soil moisture (SM). These composites, generated with variables in NCEP/NCAR Reanalysis and related datasets from NOAA/ESRL Physical Sciences Laboratory's Climate Analysis and Plotting Tools Daily Maps and Composites (Kalnay et al., 1996), are for the day of extreme events (Day-0) and the preceding two days (Day-1, Day-2) to show the large-scale configuration. We selected days of extreme events for the corresponding moisture sources as identified in the previous section. We generated these plots for land-sourced events (Figures 8–10) and GoM-sourced events (Figures 11–13) at Webster City. For these events, 9% are multi-day events with 10 two-day events for land (9%), 3 two-day events for GoM (9%), and no three-day events for either source (see Table 2). This would impact these composites primarily by elevating soil moisture in the days preceding. However, since this is such a small proportion of the total, we do not believe the impact is significant enough to change our interpretation of results.

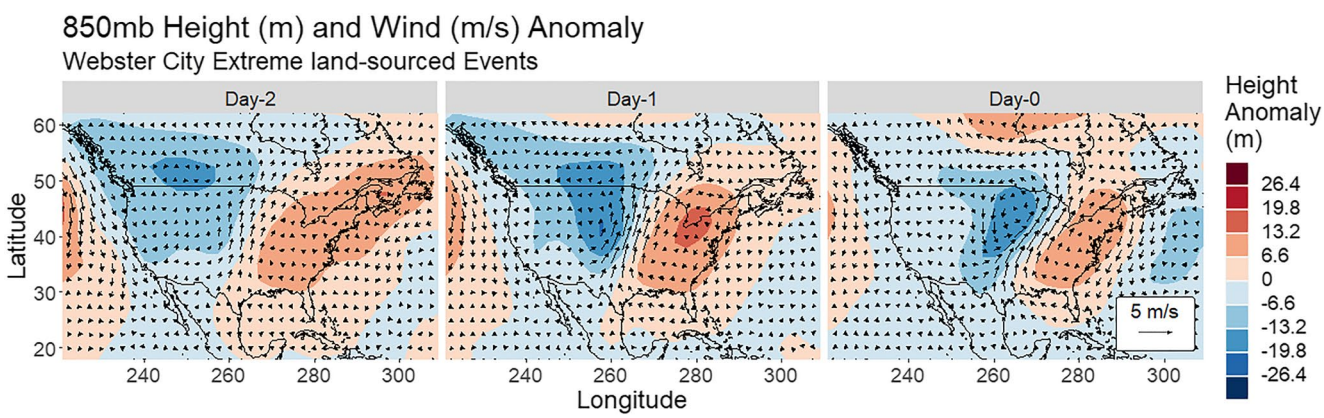

Figure 8. For extreme events at Webster City originating from land, composite maps of anomalous 850-mb geopotential height and wind from National Oceanic and Atmospheric Administrations Physical Sciences Laboratory Climate Analysis and Plotting Tools using the Daily Maps and Composites: National Centers for Environmental Prediction/NCAR Reanalysis and related datasets. Day-0 is the day of the rainfall event; Day-1 and Day-2 are 1 day and 2 days prior, respectively. Climatology used for the anomalies is 1981–2010.

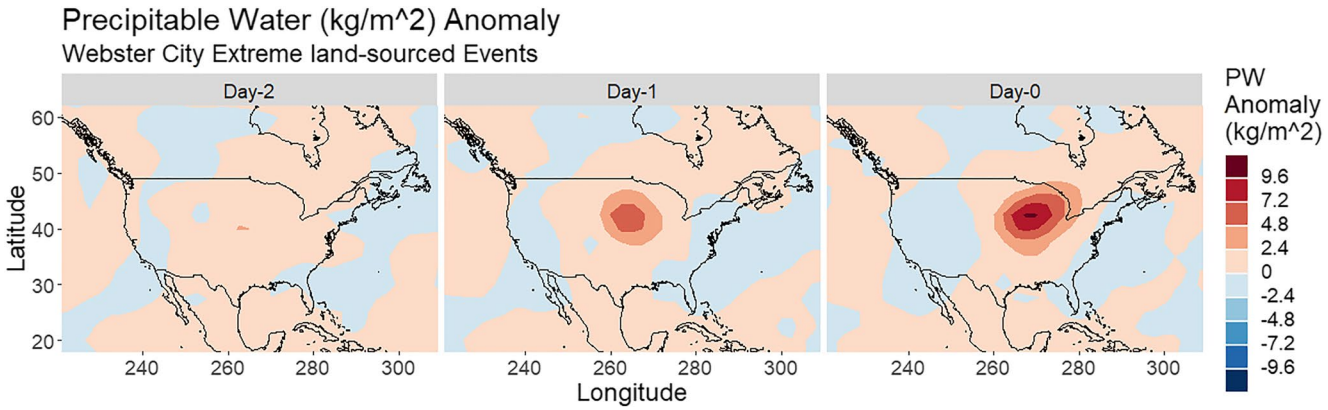

Figure 9. The same as in Figure 8, but for precipitable water.

For both land- and GoM-sourced events, there is a large low-pressure system with associated counterclockwise winds to the west of the SEPPR that begins forming two days prior (Figures 8 and 11). These systems and their winds intensify as the event approaches. The associated winds are most intense on the eastern side of the low, and the location of these winds coincides with the pathways noticed in the areal density plots (Figure 4). There are positive anomalies of PW and SM located at and surrounding the station for both land-sourced and GoM-sourced events (Figures 9, 10, 12 and 13). The region of positive PW anomalies covers the entire SEPPR and extends southward toward the Gulf of Mexico (Figures 9 and 12). The positive SM anomalies extend northwest of the station for both land- and GoM-sourced events (Figures 10 and 13).

In contrast, the GoM-sourced events have three major differences. First, the GoM-sourced events have higher magnitude anomalies - the low height anomalies are deeper (Figure 11), the winds are stronger (Figure 11), there is more PW (Figure 12), and there is more SM (Figure 13). Second, high moisture variable anomalies are more widespread for GoM-sourced events. The region of high PW anomalies spreads further in all directions, and it spreads down to the Gulf of Mexico and further into Canada (Figure 12). High SM anomalies cover a larger region, and they too spread down to the Gulf of Mexico (Figure 13). Third, the large-scale variable anomalies persist longer for the GoM-sourced events. Two days prior to the precipitation events (Day-2), the anomalies remain higher in magnitude (Figures 11–13) when compared to their land-sourced counterparts (Figures 8–10). The difference is also smaller between the anomalies on the day of the event (Day-0) and two days prior (Day-2).

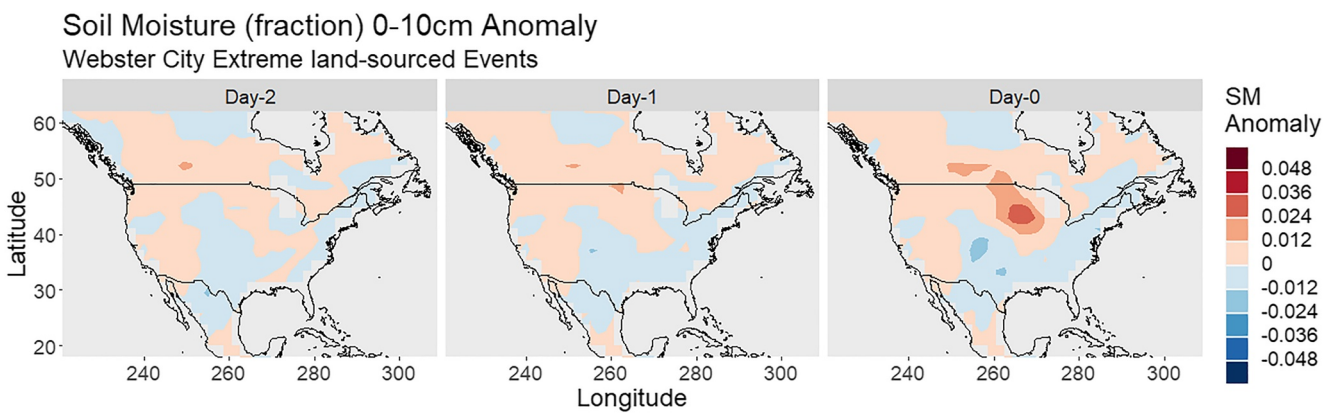

Figure 10. The same as in Figure 8, but for soil moisture.

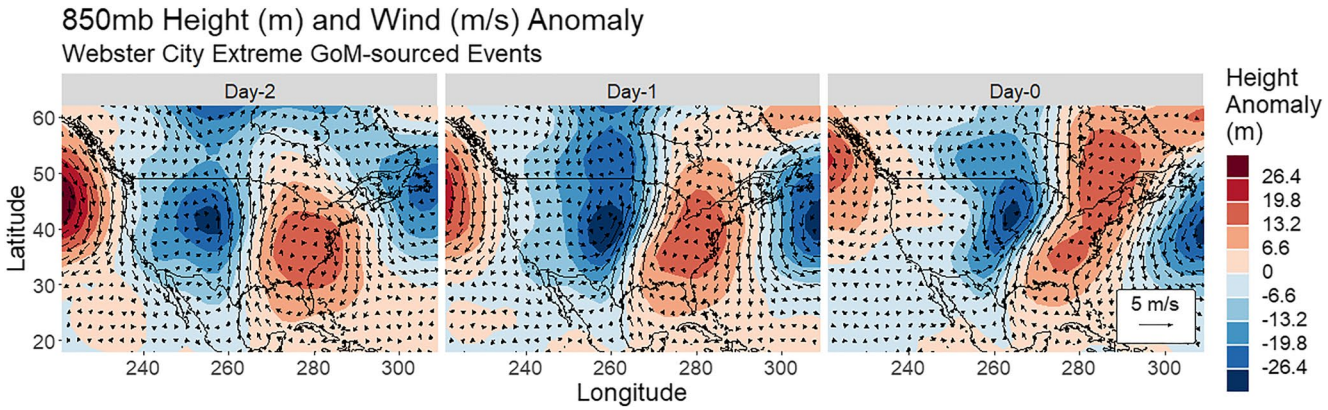

Figure 11. The same as in Figure 8, but for Gulf of Mexico-sourced events.

4.4. Large-Scale Climate Connections

Summer totals of daily rainfall amounts from land- and GoM-sourced events were averaged spatially using the seasonal total from all five stations to create a seasonal spatial average time series. This time series was correlated with gridded data sets of summer average SSTs, PDSI (Palmer, 1965), and 850-mb heights (Figures 14 and 15).

Both sources show connections and teleconnections to these large-scale variables through this analysis, though the patterns for each source differ. Land-sourced events have no significant positive correlations (Figure 14a). They have significant negative correlations in the northern Pacific Ocean and off the east coast of the U.S. For GoM-sourced events, there is a dipole of positive-negative correlations in both the north Pacific and Atlantic Oceans (Figure 15a) though the positive correlations in the northern Atlantic dipole are not significant. There are strong positive correlations up to and exceeding 0.4 to PDSI (positive PDSI indicates wet conditions) for both land- and GoM-sourced events over the western 2/3 of the U.S. (Figures 14b and 15b), but the western U.S. correlations are not significant and the land-sourced events have a larger areal extent. The GoM-sourced events have a significant positive correlation up to and exceeding 0.5 further south on the western side of the Gulf of Mexico. There are significant negative correlations up to 0.3 for land-sourced events with 850-mb heights centered over the eastern side of the SEPPR (Figure 14c). There is a large region of significant positive correlations exceeding 0.3 to the northwest of the SEPPR covering most of Canada and Alaska, and a region of positive correlations up to and exceeding 0.3 over the Caribbean. In contrast, the GoM-sourced events have significant positive correlations up to and exceeding 0.3 to the west of the SEPPR over the eastern Pacific Ocean (Figure 15c). Similarly, though, the GoM-sourced events have significant positive correlations over the Caribbean. There are no significant negative correlations for the GoM-sourced events.

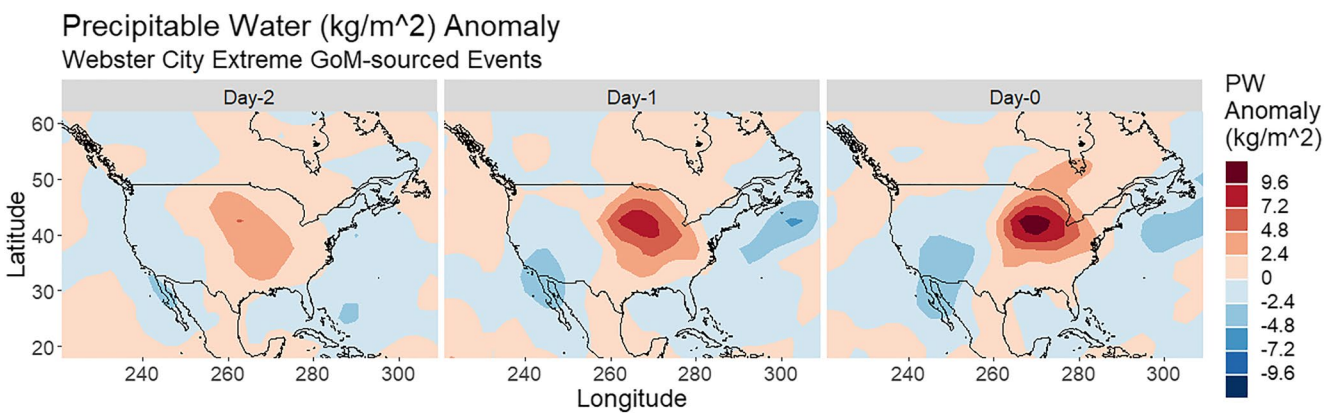

Figure 12. The same as in Figure 9, but for Gulf of Mexico -sourced events.

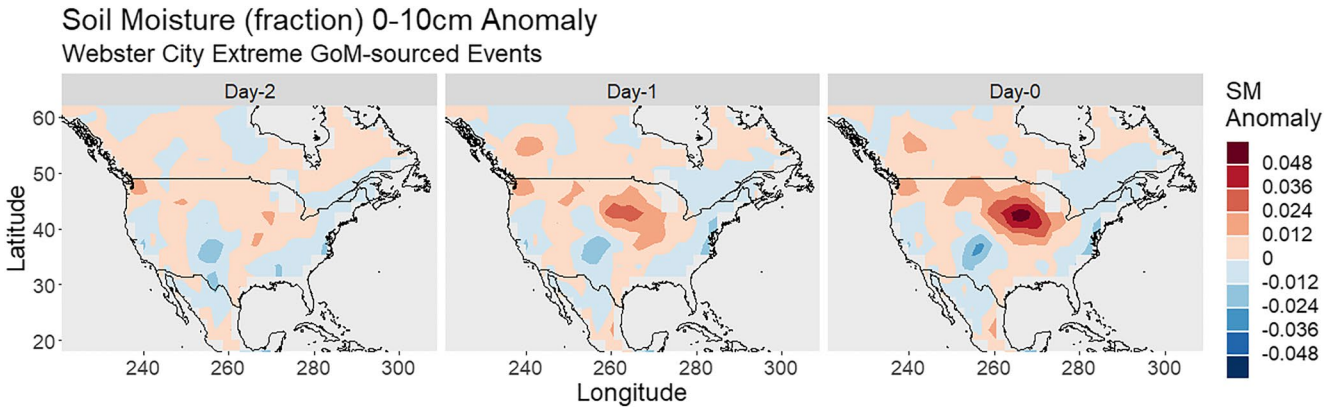

Figure 13. The same as in Figure 10, but for Gulf of Mexico -sourced events.

4.5. Trend Analysis of Rain Amount by Source

We tested the trends in the time series of the seasonal rainfall totals from the land-sourced events at each of the five stations. This was performed for both rain and extreme events. We used the Mann-Kendall trend test (Helsel et al., 2020; Mann, 1945) to test if a trend exists. The only significant trend at a 95% level or greater was that of extreme events at Minot which was significant at 97% level. We performed the same test on the time series of the percentage of trajectories originating from the land from each of the five stations. This was also performed for both rain and extreme events. None of the slopes were significant. P-values and slopes can be found in Table S2 in Supporting Information S1.

5. Summary and Discussion

In this study, we used a Lagrangian parcel-tracking model, HYSPLIT, to calculate back trajectories of summer precipitation events to determine primary moisture sources. Trajectories were calculated for precipitation events at five representative stations spaced across the SEPPR and representing all four Level III Ecoregions coincident with the SEPPR. Trajectories were calculated for both rain and extreme events with the 90th percentile separating the two. We can draw the following conclusions from our results.

Land is the primary source of moisture for both rain and extreme events in summer across all stations represented (Figure 3) which agrees with previous studies which examined moisture sources for precipitation events that included parts of the SEPPR (Brubaker et al., 2001; Dirmeyer & Brubaker, 1999; Dirmeyer & Kinter III, 2010). This indicates that soil moisture and moisture recycling play an important role in summer precipitation generation in the region. Recall that previous studies have found a connection between soil moisture and summer precipitation (Koster et al., 2004; Meng & Quiring, 2010; Yoon & Leung, 2015). The implication of this is that changes in the evaporation to precipitation ratio would likely have significant impacts on moisture available for the SEPPR. Increases in average temperature and climate variability due to climate change would mean more moisture evaporates instead of infiltrating and therefore less soil moisture availability causing a decrease in the precipitation over the longer term.

The Gulf of Mexico is the secondary source of moisture for precipitation events, and stations further to the southeast had a stronger influence from it (Figure 3). Our results provide evidence that the GPLLJ and "Maya Express" AR, strong spring and summer circulation features in this region (Gimeno et al., 2016; Higgins et al., 1997; Knippertz & Wernli, 2010; Lavers & Villarini, 2013), play a crucial role in the moisture transport to the region, similar to that found by Song et al. (2019). Examining the trajectory density maps for land- and GoM-sourced events (Figures 4 and 5), we notice moisture pathways frequently coming from the south along a pathway common for the GPLLJ and "Maya Express". The GPLLJ can bring moisture from the southern Great Plains to the SEPPR (Pu et al., 2016). In addition, if underlying soil moisture is anomalously high, the GPLLJ would intensify (Li et al., 2016, 2017) and increase moisture transport to the SEPPR. Extreme events showed an even stronger

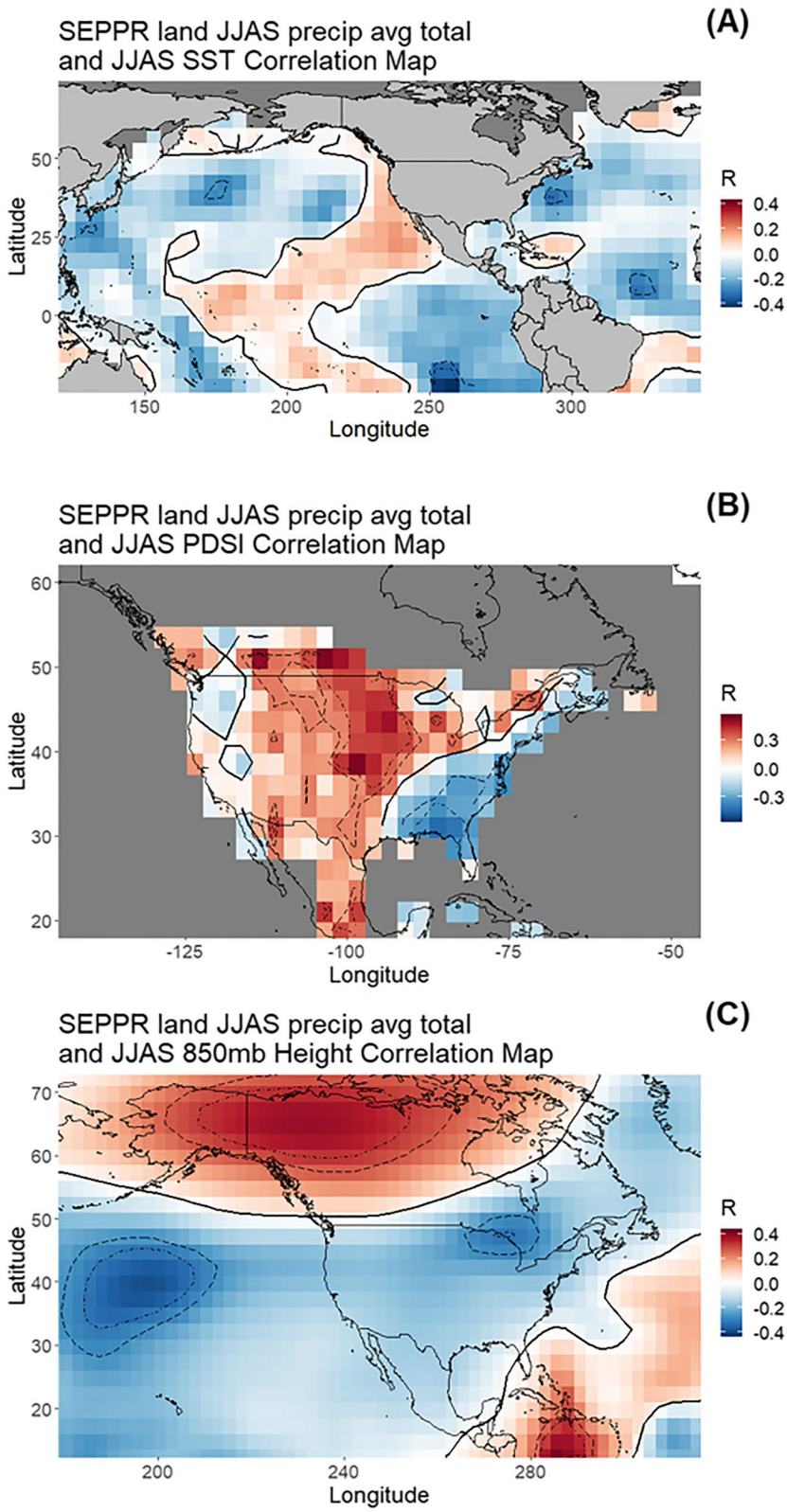

Figure 14. Correlation map between the summer total precipitation from land-sourced events spatially averaged from all five stations and (a) summer sea surface temperatures (1979–2017), (b) summer Palmer Drought Severity Index (1979–2014), and (c) summer 850-mb heights (1979–2019). Correlation coefficient values significant at a 90% and 95% level have been outlined with long dashed and dot-dashed contours, respectively. The thick, solid contour demarcates the division between positive and negative correlation values.

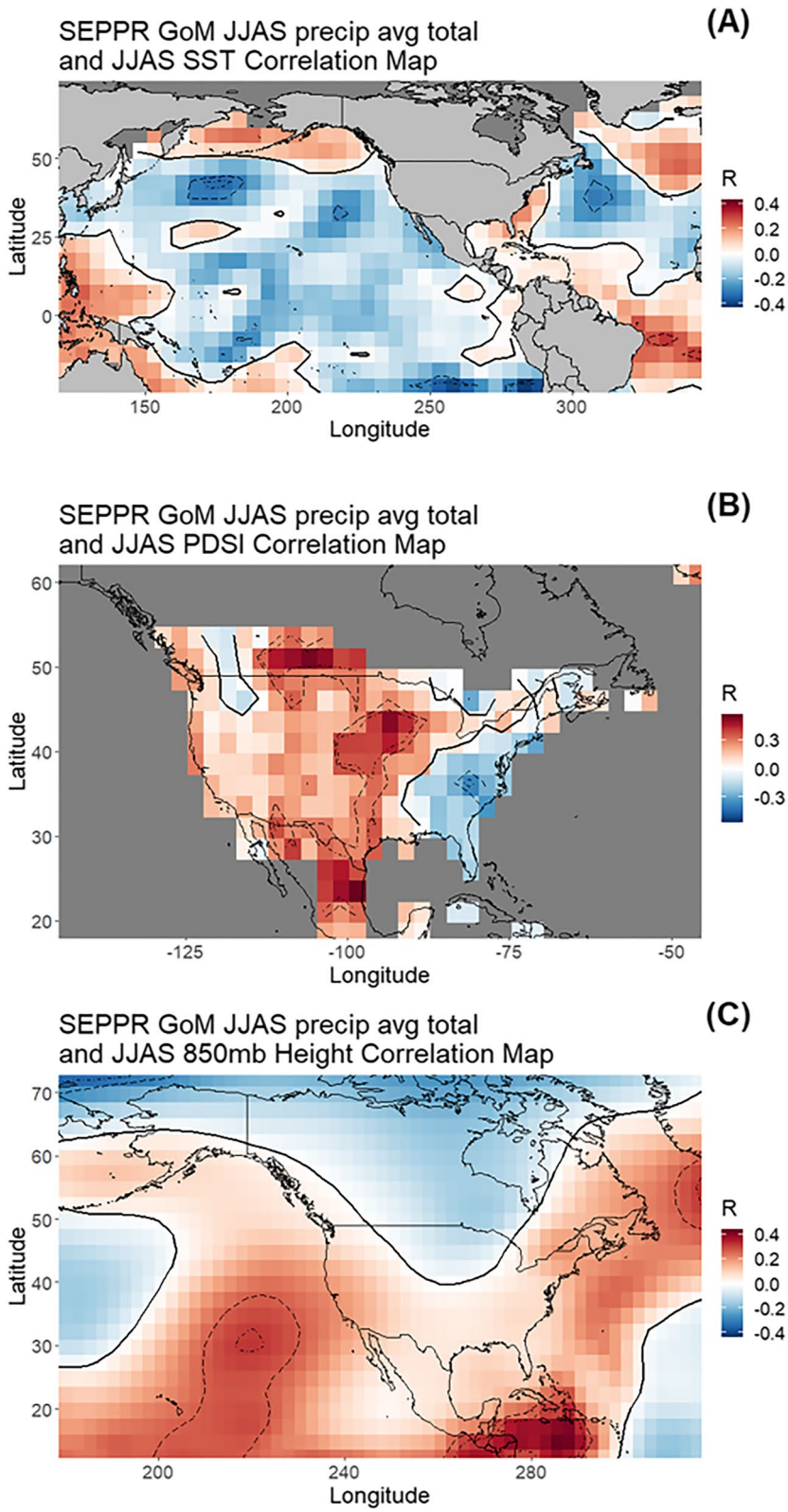

Figure 15. As in Figure 14, but for trajectories originating from Gulf of Mexico.

influence from the south which is in line with other studies that have shown that heavy rainfall and flooding events were significantly influenced by moisture transport from the "Maya Express" (Knippertz & Wernli, 2010; Lavers & Villarini, 2013).

GoM-sourced rain events are higher in precipitation amount with more variability in amount than land-sourced rain events (Figure 6). We hypothesize that GoM-sourced events bring more moisture with a longer travel distance that adds to the variability in amount, while land-sourced events tend to be more localized thunderstorms with less moisture. This phenomenon of higher precipitation and variability for GoM-sourced events is not present for extreme events (Figure 7) which suggests that for extreme, land-sourced events, their local reach can be just as potent in producing an extreme event as the GoM-sourced back trajectories. Overall, though, GoM-sourced events produce more rainfall than land-sourced events. Additionally, GoM-sourced events have large-scale setups that present up to a day earlier than land-sourced events (Figures 8–13). Further, GoM-sourced events present with higher-magnitude large-scale variable anomalies (Figures 8–13). We believe this indicates that GoM-sourced events include stronger and larger systems such as MCSs, supercell thunderstorms, and tropical storms (Song et al., 2019, 2021 found that MCSs had a strengthened GPLLJ) while land-sourced events tend to be more localized thunderstorms (higher localized soil moisture, natural or irrigation induced, has been shown to increase localized precipitation [de Vrese & Stacke, 2020; Findell et al., 2011]).

In general, we observe large-scale climate connections through correlation maps (Figures 14 and 15) that demonstrate there is a distinct coupling between the land, atmosphere, and ocean that influences summer precipitation in the SEPPR, something that has been documented in other works (e.g., Dirmeyer & Kinter III, 2009). Land-sourced events show a connection to the northern Pacific and northwest Atlantic Oceans (i.e., the ocean), soil moisture (as a component of PDSI) over the central U.S. and locally over SEPPR (i.e., land), and low-pressure systems over the SEPPR and high-pressure systems over the Caribbean (i.e., the atmosphere). GoM-sourced events have connections to SSTs in the north Pacific and Atlantic Oceans (i.e., the ocean), soil moisture over the central U.S. and in northern Mexico (i.e., land), and high 850-mb heights in the eastern Pacific Ocean (i.e., the atmosphere). GoM-sourced events, just like land-sourced events, show connections to high 850-mb heights in the Caribbean - this may be a reflection of a strengthened Bermuda High. These large-scale connections may be exploited to make more accurate seasonal forecasts of precipitation. For example, forecasters can examine soil moisture or PDSI maps and use them as a component of their forecast decision - high anomalies in the regions with connections identified in this manuscript would increase their precipitation probability forecast. Another possibility would be to use these large-scale connections to develop a statistical model for precipitation forecasts at a regional level (e.g., county) similar in design to the forecast model in Abel et al. (2020).

In summary, the land is the predominant source for precipitation events in the SEPPR indicating moisture recycling is an important mechanism for water availability in the region. The Gulf of Mexico also plays a significant role in providing moisture for precipitation with the GPLLJ and "Maya Express" likely being major modes of moisture transport. Our findings regarding the role of land and the GoM in producing organized moisture trajectories for rainfall during summer in this region is quite clear. These findings can serve as insight for further studies of moisture origin for the SEPPR in other seasons. They can also assist in seasonal precipitation forecasts, as mentioned above. Another possible avenue for further research would be comparing our results to trajectories for dry days - the "mean state". While our results assist in precipitation forecasts, results for the mean state would help in prediction of long term drought.

Data Availability Statement

The data that support the findings of this study are openly available at the following URL/DOI. Global Historical Climate Network - Daily: https://www.ncdc.noaa.gov/ghcn-daily-description. Hybrid Single-Particle Lagrangian Integrated Trajectory (HYSPLIT) model: https://www.ready.noaa.gov/HYSPLIT.php. North American Regional Reanalysis: https://www.ready.noaa.gov/archives.php; ftp://ftp.arl.noaa.gov/narr. NOAA PSL Anomaly Composites: https://psl.noaa.gov/cgi-bin/data/getpage.pl. IRI Data Library: https://iridl.ldeo.columbia.edu/. NOAA PSL Climate Data Repository: https://psl.noaa.gov/repository/a/psdgrids.

Acknowledgments
The authors gratefully acknowledge funding for this research from National Science Foundation (NSF) grant #1243270 - "Linking near-term future changes in weather and hydroclimate in western North America to adaptation for ecosystem and water management". Andrea J. Ray was funded by the NOAA Physical Sciences Laboratory. Publication of this article was funded by the University of Colorado Boulder Libraries Open Access Fund. The authors gratefully acknowledge the NOAA Air Resources Laboratory (ARL) for the provision of the HYSPLIT transport and dispersion model used in this publication. Composite image data provided by the NOAA/ESRL Physical Sciences Laboratory, Boulder Colorado from their website at https://psl.noaa.gov/cgi-bin/data/getpage.pl. We thank Bruce Millett for the original PPR shapefile and Angela Boag for PPR shapefile modification. We thank an anonymous reviewer whose comments helped to improve this manuscript.

References

Abel, B., Rajagopalan, B., & Ray, A. (2020). A predictive model for seasonal pond counts in the United States Prairie Pothole Region using large-scale climate connections. *Environmental Research Letters*, *15*, 044019. https://doi.org/10.1088/1748-9326/ab7465

Batt, B., Anderson, M., Anderson, C., & Caswell, F. (1989). The use of prairie potholes by North American ducks. In A. van der Valk (Ed.), *Northern prairie wetlands* (p. 204–227). Iowa State University Press.

Benton, G., & Estoque, M. (1954). Water-vapor transfer over the North American continent. *Journal of the Atmospheric Sciences*, *11*(6), 462–477. https://doi.org/10.1175/1520-0469(1954)011<0462:wvtotn>2.0.co;2

Bracken, C., Rajagopalan, B., Alexander, M., & Gangopadhyay, S. (2015). Spatial variability of seasonal extreme precipitation in the western United States. *Journal of Geophysical Research: Atmospheres*, *120*(10), 4522–4533. https://doi.org/10.1002/2015JD023205

Bromley, G., Gerken, T., Prein, A., & Stoy, P. (2020). Recent trends in the near-surface climatology of the northern north American great plains. *Journal of Climate*, *33*(2), 461–475. https://doi.org/10.1175/JCLI-D-19-0106.1

Brubaker, K., Dirmeyer, P., Sudradjat, A., Levy, B., & Bernal, F. (2001). A 36-yr climatological description of the evaporative sources of warm-season precipitation in the Mississippi River basin. *Journal of Hydrometeorology*, *2*(6), 537–557. https://doi.org/10.1175/1525-7541(2001)002<0537:aycdot>2.0.co;2

Conant, R., Kluck, D., Anderson, M., Badger, A., Boustead, B., Derner, J., et al. (2018). Northern Great Plains. In D. Reidmiller (Ed.), *Impacts, risks, and adaptation in the United States: Fourth national climate assessment* (Vol. ii, pp. 941–986). U.S. Global Change Research Program. https://doi.org/10.7930/NCA4.2018.CH22

Dahl, T. (2014). *Status and trends of prairie wetlands in the United States 1997 to 2009 (Report)*. Department of the Interior; Fish and Wildlife Service, Ecological Services. Retrieved from https://www.fws.gov/wetlands/Documents/Status-and-Trends-of-Prairie-Wetlands-in-the-United-States-1997-to-2009.pdf

Dai, A., Trenberth, K. E., & Qian, T. (2004). A global dataset of Palmer drought severity index for 1870–2002: Relationship with soil moisture and effects of surface warming. *Journal of Hydrometeorology*, *5*(6), 1117–1130. https://doi.org/10.1175/JHM-386.1

de Vrese, P., & Stacke, T. (2020). Irrigation and hydrometeorological extremes. *Climate Dynamics*, *55*, 1521–1537. https://doi.org/10.1007/s00382-020-05337-9

Debbage, N., Miller, P., Poore, S., Morano, K., Mote, T., & Shepherd, J. M. (2017). A climatology of atmospheric river interactions with the southeastern United States coastline. *International Journal of Climatology*, *37*(11), 4077–4091. https://doi.org/10.1002/joc.5000

Dirmeyer, P., & Brubaker, K. (1999). Contrasting evaporative moisture sources during the drought of 1988 and the flood of 1993. *Journal of Geophysical Research: Atmospheres*, *104*(D16), 19383–19397. https://doi.org/10.1029/1999JD900222

Dirmeyer, P., & Kinter, III, J. (2009). The "Maya Express": Floods in the U.S. Midwest. *Eos*, *90*(12), 101–102. https://doi.org/10.1029/2009EO120001

Dirmeyer, P., & Kinter, III, J. (2010). Floods over the U.S. Midwest: A regional water cycle perspective. *Journal of Hydrometeorology*, *11*(5), 1172–1181. https://doi.org/10.1175/2010JHM1196.1

Draxler, R. (1999). *HYSPLIT4 user's guide (NOAA Technical Memorandum No. ERL ARL-230)*. NOAA Air Resources Laboratory. Retrieved from https://www.arl.noaa.gov/wp_arl/wp-content/uploads/documents/reports/arl-230.pdf

Draxler, R., & Hess, G. (1997). *Description of the HYSPLIT_4 modeling system (NOAA Technical Memorandum No. ERL ARL-224)*. NOAA Air Resources Laboratory. Retrieved from https://www.arl.noaa.gov/wp_arl/wp-content/uploads/documents/reports/arl-224.pdf

Draxler, R., & Hess, G. (1998). An overview of the HYSPLIT_4 modeling system of trajectories, dispersion, and deposition. *Australian Meteorological Magazine*, *47*, 295–308.

Durre, I., Menne, M., Gleason, B., Houston, T., & Vose, R. (2010). Comprehensive automated quality assurance of daily surface observations. *Journal of Applied Meteorology and Climatology*, *49*(8), 1615–1633. https://doi.org/10.1175/2010JAMC2375.1

Durre, I., Menne, M., & Vose, R. (2008). Strategies for evaluating quality assurance procedures. *Journal of Applied Meteorology and Climatology*, *47*(6), 1785–1791. https://doi.org/10.1175/2007JAMC1706.1

Easterling, D., Arnold, J., Knutson, T., Kunkel, K., LeGrande, A., Leung, L., et al. (2017). Precipitation change in the United States. In D. Wuebbles, D. Fahey, K. Hibbard, D. Dokken, B. Stewart, & T. Maycock (Eds.), *Climate science special report: Fourth national climate assessment* (Vol. i, pp. 207–230). U.S. Global Change Research Program. https://doi.org/10.7930/J0H993CC

Findell, K., Gentine, P., Lintner, B., & Kerr, C. (2011). Probability of afternoon precipitation in eastern United States and Mexico enhanced by high evaporation. *Nature Geoscience*, *4*(7), 434–439. https://doi.org/10.1038/NGEO1174

Fritsch, J., Kane, R., & Chelius, C. (1986). The contribution of mesoscale convective weather systems to the warm-season precipitation in the United States. *Journal of Applied Meteorology and Climatology*, *25*(10), 1333–1345. https://doi.org/10.1175/1520-0450(1986)025<1333:tcomcw>2.0.co;2

Gimeno, L., Dominguez, F., Nieto, R., Trigo, R., Drumond, A., Reason, C., et al. (2016). Major mechanisms of atmospheric moisture transport and their role in extreme precipitation events. *Annual Review of Environment and Resources*, *41*, 117–141. https://doi.org/10.1146/annurev-environ-110615-085558

Gustafsson, M., Rayner, D., & Chen, D. (2010). Extreme rainfall events in southern Sweden: Where does the moisture come from? *Tellus A: Dynamic Meteorology and Oceanography*, *62*(5), 605–616. https://doi.org/10.1111/j.1600-0870.2010.00456.x

Haberlie, A., & Ashley, W. (2019). A Radar-based climatology of mesoscale convective systems in the United States. *Journal of Climate*, *32*(5), 1591–1606. https://doi.org/10.1175/JCLI-D-18-0559.1

Hayashi, M., Kamp, G., & Rosenberry, D. (2016). Hydrology of prairie wetlands: Understanding the Integrated surface-water and Groundwater processes. *Wetlands*, *36*, 237–254. https://doi.org/10.1007/s13157-016-0797-9

Helsel, D., Hirsch, R., Ryberg, K., Archfield, S., & Gilroy, E. (2020). Statistical methods in water resources. *Statistical methods in water resources (Report No. 4-A3)*. U.S. Geological Survey. https://doi.org/10.3133/tm4A3

Higgins, R., Yao, Y., Yarosh, E., Janowiak, J., & Mo, K. (1997). Influence of the great plains low-level Jet on Summertime precipitation and moisture transport over the Central United States. *Journal of Climate*, *10*(3), 481–507. https://doi.org/10.1175/1520-0442(1997)010<0481:iotgpl>2.0.co;2

Izquierdo, R., Avila, A., & Alarcón, M. (2012). Trajectory statistical analysis of atmospheric transport patterns and trends in precipitation chemistry of a rural site in NE Spain in 1984–2009. *Atmospheric Environment*, *61*, 400–408. https://doi.org/10.1016/j.atmosenv.2012.07.060

Jana, S., Rajagopalan, B., Alexander, M., & Ray, A. (2018). Understanding the dominant sources and tracks of moisture for summer rainfall in the southwest United States. *Journal of Geophysical Research: Atmospheres*, *123*(10), 4850–4870. https://doi.org/10.1029/2017JD027652

Johnson, W., & Poiani, K. (2016). Climate change effects on prairie pothole wetlands: Findings from a Twenty-five Year numerical modeling Project. *Wetlands*, *36*, 273–285. https://doi.org/10.1007/s13157-016-0790-3

Johnson, W., Millett, B., Gilmanov, T., Voldseth, R., Guntenspergen, G., & Naugle, D. (2005). Vulnerability of northern prairie wetlands to climate change. *BioScience*, *55*, 863. https://doi.org/10.1641/0006-3568(2005)055[0863:vonpwt]2.0.co;2

Johnson, W., Werner, B., Guntenspergen, G., Voldseth, R., Millett, B., Naugle, D., et al. (2010). Prairie wetland Complexes as landscape functional Units in a changing climate. *BioScience*, *60*, 128–140. https://doi.org/10.1525/bio.2010.60.2.7

Jorba, O., Perez, C., Rocadenbosch, F., & Baldasano, J. (2004). Cluster Analysis of 4-day back trajectories arriving in the Barcelona area, Spain, from 1997 to 2002. *Journal of Applied Meteorology and Climatology*, *43*(6), 887–901. https://doi.org/10.1175/1520-0450(2004)043<0887:caodbt>2.0.co;2

Kalnay, E., Kanamitsu, M., Kistler, R., Collins, W., Deaven, D., Gandin, L., et al. (1996). The NCEP/NCAR 40-year reanalysis project. *Bulletin of the American Meteorological Society*, *77*(3), 437–471. https://doi.org/10.1175/1520-0477(1996)077<0437:tnyrp>2.0.co;2

Kantrud, H., Krapu, G., & Swanson, G. (1989). *Prairie basin wetlands of the Dakotas: A community profile (Biological Report No. 85(7.28))*. U.S. Fish and Wildlife Service. Retrieved from https://pubs.er.usgs.gov/publication/2000127

Kaplan, A., Cane, M., Kushnir, Y., Clement, A., Blumenthal, M., & Rajagopalan, B. (1998). Analyses of global sea surface temperature 1856–1991. *Journal of Geophysical Research*, *103*, 18567–18589. https://doi.org/10.1029/97JC01736

Knippertz, P., & Wernli, H. (2010). A Lagrangian climatology of tropical moisture exports to the northern hemispheric extratropics. *Journal of Climate*, *23*(4), 987–1003. https://doi.org/10.1175/2009JCLI3333.1

Koster, R., Dirmeyer, P., Guo, Z., Bonan, G., Chan, E., Cox, P., et al. (2004). Regions of strong coupling between soil moisture and precipitation. *Science*, *305*(5687), 1138–1140. https://doi.org/10.1126/science.1100217

Lavers, D. A., & Villarini, G. (2013). Atmospheric rivers and flooding over the central United States. *Journal of Climate*, *26*(20), 7829–7836. https://doi.org/10.1175/JCLI-D-13-00212.1

Li, L., Schmitt, R., & Ummenhofer, C. (2017). The role of the subtropical north Atlantic water cycle in recent us extreme precipitation events. *Climate Dynamics*, *50*, 1291–1305. https://doi.org/10.1007/s00382-017-3685-y

Li, L., Schmitt, R., Ummenhofer, C., & Karnauskas, K. (2016). Implications of north Atlantic Sea surface salinity for summer precipitation over the U.S. midwest: Mechanisms and predictive value. *Journal of Climate*, *29*(9), 3143–3159. https://doi.org/10.1175/JCLI-D-15-0520.1

Mann, H. (1945). Nonparametric tests against trend. *Econometrica*, *13*(3), 245–259. https://doi.org/10.2307/1907187

Meng, L., & Quiring, S. (2010). Observational relationship of sea surface temperatures and precedent soil moisture with summer precipitation in the U.S. Great Plains. *International Journal of Climatology*, *30*(6), 884–893. https://doi.org/10.1002/joc.1941

Menne, M., Durre, I., Vose, R., Gleason, B., & Houston, T. (2012). An overview of the global historical climatology Network-daily Database. *Journal of Atmospheric and Oceanic Technology*, *29*(7), 897–910. https://doi.org/10.1175/JTECH-D-11-00103.1

Mesinger, F., DiMego, G., Kalnay, E., Mitchell, K., Shafran, P., Ebisuzaki, W., et al. (2006). North American regional reanalysis. *Bulletin of the American Meteorological Society*, *87*(3), 343–360. https://doi.org/10.1175/BAMS-87-3-343

Millett, B., Johnson, W., & Guntenspergen, G. (2009). Climate trends of the North American prairie pothole region 1906–2000. *Climatic Change*, *93*, 243–267. https://doi.org/10.1007/s10584-008-9543-5

Mo, K., Chelliah, M., Carrera, M., Higgins, R., & Ebisuzaki, W. (2005). Atmospheric moisture transport over the United States and Mexico as Evaluated in the NCEP regional reanalysis. *Journal of Hydrometeorology*, *6*(5), 710–728. https://doi.org/10.1175/JHM452.1

National Oceanic and Atmospheric Administration. (2021). *Constant pressure charts: 850 mb*. Retrieved from https://www.weather.gov/jetstream/850mbs

Omernik, J., & Griffith, G. (2014). Ecoregions of the conterminous United States: Evolution of a hierarchical spatial framework. *Environmental Management*, *54*, 1249–1266. https://doi.org/10.1007/s00267-014-0364-1

Palmer, W. (1965). *Meteorological drought (research paper No. No. 45)*. U.S. Dept. of Commerce. Retrieved from https://www.ncdc.noaa.gov/temp-and-precip/drought/docs/palmer.pdf

Pomeroy, J., Gray, D., Shook, K., Toth, B., Essery, R., Pietroniro, A., & Hedstrom, N. (1998). An evaluation of snow accumulation and ablation processes for land surface modelling. *Hydrological Processes*, *12*, 2339–2367. https://doi.org/10.1002/(sici)1099-1085(199812)12:15<2339::aid-hyp800>3.0.co;2-1

Pu, B., Fu, R., Dickinson, R., & Fernando, D. (2016). Why do summer droughts in the Southern Great Plains occur in some la niña years but not others? *Journal of Geophysical Research - D: Atmospheres*, *121*, 1120–1137. https://doi.org/10.1002/2015JD023508

Reynolds, R., & Smith, T. (1994). Improved global sea surface temperature analyses using optimum interpolation. *Journal of Climate*, *7*, 929–948. https://doi.org/10.1175/1520-0442(1994)007<0929:igssta>2.0.co;2

Rosenberry, D. (2003). Climate of the Cottonwood Lake area. In T. Winter (Ed.), *Hydrological, chemical, and biological characteristics of a prairie pothole wetland complex under highly variable climate conditions - the cottonwood lake area, east-central North Dakota* (p. 25–34). U.S. Geological Survey. https://doi.org/10.3133/pp1675

Schumacher, R., & Johnson, R. (2006). Characteristics of U.S. Extreme rain events during 1999–2003. *Weather and Forecasting*, *21*(1), 69–85. https://doi.org/10.1175/WAF900.1

Smith, A., Stoudt, J., & Gallop, J. (1964). Prairie pothole wetlands and marshes. In J. Linduska (Ed.), *Waterfowl tomorrow* (p. 39–50). U.S. Government Printing Office.

Song, F., Feng, Z., Leung, L., Houze, Jr, R., Wang, J., Hardin, J., & Homeyer, C. (2019). Contrasting spring and summer large-scale environments associated with mesoscale convective systems over the U.S. Great plains. *Journal of Climate*, *32*(20), 6749–6767. https://doi.org/10.1175/JCLI-D-18-0839.1

Song, F., Feng, Z., Leung, L., Pokharel, B., Wang, S.-Y. S., Chen, X., et al. (2021). Crucial roles of eastward propagating environments in the summer mcs initiation over the U.S. great plains. *Journal of Geophysical Research: Atmospheres*, *126*(16). https://doi.org/10.1029/2021JD034991

Stein, A., Draxler, R., Rolph, G., Stunder, B., Cohen, M., & Ngan, F. (2015). NOAA's HYSPLIT atmospheric transport and dispersion modeling system. *Bulletin of the American Meteorological Society*, *96*(12), 2059–2077. https://doi.org/10.1175/BAMS-D-14-00110.1

Trenberth, K. (1998). Atmospheric moisture residence times and cycling: Implications for rainfall rates and climate change. *Climatic Change*, *39*, 667–694. https://doi.org/10.1023/A:1005319109110

Vecchia, A. (2008). Climate simulation and flood risk analysis for 2008-40 for Devils Lake, North Dakota. *Climate simulation and flood risk analysis for 2008-40 for Devils lake, north Dakota (Scientific Investigations Report No. 2008–5011)*. U.S. Geological Survey. https://doi.org/10.3133/sir20085011

Winter, T. (2000). The vulnerability of wetlands to climate change: A hydrologic landscape perspective. *Journal of the American Water Resources Association*, *36*, 305–311. https://doi.org/10.1111/j.1752-1688.2000.tb04269.x

Yocum, H., & Ray, A. (2019). Climate information to support wildlife management in the North Central United States. *Regional Environmental Change*, *19*, 1187–1199. https://doi.org/10.1007/s10113-019-01474-y

Yoon, J., & Leung, L. (2015). Assessing the relative influence of surface soil moisture and enso sst on precipitation predictability over the contiguous United States. *Geophysical Research Letters*, *42*(12), 5005–5013. https://doi.org/10.1002/2015GL064139